Comparison of Model-Fitting Kinetics for Predicting the Cure Behavior of Commercial Phenol–Formaldehyde Resins

Jinwu Wang, Marie-Pierre G. Laborie, Michael P. Wolcott

Wood Materials and Engineering Laboratory, Department of Civil and Environmental Engineering, Washington State University, Pullman, Washington 99164-1806

Received 8 November 2005; accepted 2 June 2006
DOI 10.1002/app.24855
Published online 23 April 2007 in Wiley InterScience (www.interscience.wiley.com).

ABSTRACT: Phenol–formaldehyde (PF) resins have been the subject of many model-fitting cure kinetic studies, yet the best model for predicting PF dynamic and isothermal cure has not been established. The objective of this research is to compare and contrast several commonly used kinetic models for predicting degree of cure and cure rate of PF resins. Toward this objective, the *n*th-order Borchardt–Daniels (*n*th-BD), ASTM E698 (E698), autocatalytic Borchardt–Daniels (Auto-BD), and modified autocatalytic methods (M-Auto) are evaluated on two commercial PF resins containing different molecular weight distributions and thus cure behaviors. The *n*th-BD, E698, and M-Auto methods all produce comparable values of activation energies, while Auto-BD method yields aberrant values. For dynamic cure prediction, all models fail to predict reaction rate, while degree of cure is reasonably well predicted with all three methods. As a whole, the *n*th-BD method best predicts degree of cure for both resins as assessed by mean squared error of prediction. © 2007 Wiley Periodicals, Inc. J Appl Polym Sci 105: 1289–1296, 2007

Key words: resins; activation energy; modeling; kinetics (polymer); differential scanning calorimetry (DSC)

INTRODUCTION

Several hot-pressing models of engineered wood-based composites have been developed to predict properties such as moisture content and internal pressure during mat-solidification in the past decades.[1–4] Such models are important to design and optimize hot-pressing parameters during the manufacture of engineered wood-based composites. During panel consolidation, the heat of resin polymerization plays an important role. Yet hot-pressing models have either used an arbitrary kinetic model or have not incorporated the resin cure kinetics,[1–4] hence limiting their application. To improve the accuracy of hot-pressing models, cure kinetics needs to be incorporated. During a differential scanning calorimetry (DSC) temperature scan phenol–formaldehyde (PF) resoles typically exhibit two exotherms.[5] Although a subject of controversy, the first exotherm is often ascribed to hydroxymethylphenols formation and condensation, while the second exotherm is attributed to dimethylene ether linkages decomposition into methylene linkages between phenolic moieties.[5] To model resin cure kinetics, model-fitting (MF)[6] and model-free kinetics[7] can be used in combination with DSC.[8] For commercial PF resins, model-free kinetics has recently demonstrated excellent modeling and prediction abilities for both degree of cure and reaction rate during dynamic and isothermal cure.[7] However, model-free kinetics involves complex computations that may not be easily implemented in a comprehensive hot-pressing model. Indeed, hot-pressing models require solving simultaneously two governing partial differential equations, one on heat transfer and one on mass transfer.[1] As a result, an explicit cure kinetic model can be more easily incorporated into the solving process. In contrast, MF methods assume a definite reaction model, facilitating simple computations with kinetic parameters such as activation energy, reaction order, and pre-exponential factor. As such, they remain of interest when an approximate prediction of cure development is needed, and will be easily incorporated into a hot-pressing model. In fact, MF kinetics has long been used to characterize and compare the cure kinetics of different PF resins.[9–12] In particular, the *n*th order model with the Borchardt–Daniels[13] and the ASTM E698[14] methods have been widely utilized. Yet different kinetic methods often generate different kinetic parameters.[15] For instance, the *n*th order with the Borchardt–Daniels method was reported to yield activation energy values that are 30% higher than those obtained with the Ozawa or Kissinger equations used in ASTM E698.[15] These observations raise a concern

Correspondence to: M.-P. G. Laborie (mlaborie@wsu.edu).

Journal of Applied Polymer Science, Vol. 105, 1289–1296 (2007)

about which MF method is best suited to model the cure kinetics of different commercial resins including the PF varieties studied in this research. More importantly, the prediction ability of MF methods for phenolic resin cure has not been established. The choice of an MF method to predict PF cure kinetics for incorporating into hot-pressing models is, therefore, not evident. In this perspective, the objective of this study is to determine and compare the suitability of four MF kinetic methods to model and predict the cure kinetics of PF resins. The specific models studied include the *n*th order with Borchardt–Daniels, autocatalytic model with Borchardt–Daniels, ASTM E698, and modified autocatalytic methods.[6]

EXPERIMENTAL

Materials

Two PF resole resins tailored for use in face and core layers of oriented strand board (OSB) production were obtained from a commercial source.[7] The face resin displayed a weight-average molecular weight (M_w) of 621 g/mol and a polydispersity (M_w/M_n) of 1.4. This resin was subsequently identified as PF-low.[7] The core resin possessed a $M_w = 6576$ g/mol and $M_w/M_n = 1.72$ and was labeled as PF-high.[7] Resin solids contents for the PF-low and PF-high resins were 54.5 and 45.0%, respectively.[7] In addition, elemental analysis[16] showed the presence of 3.7 and 3.9 wt % nitrogen for PF-high and PF-low respectively, suggesting the presence of urea in both resins.

Differential scanning calorimetry

A Mettler-Toledo DSC 822e was used to perform dynamic and isothermal cure experiments. Approximately 13.5 mg of resin was placed in a 30 μL high pressure gold-plated crucible. Dynamic temperature scans were conducted from 25 to 250°C at four heating rates: 2, 5, 10, and 20°C/min. In all DSC scans, nitrogen was used as a purge gas at a flow rate of 80 mL/min. Six replicate measurements were performed for each heating rate. Four randomly selected measurements were used to extract kinetic parameters and remaining two measurements were used to compare with predictions. In addition, the first replicate was rescanned at 10°C/min immediately following the first scan to assure complete cure. Both degree of cure (α) and reaction rate ($d\alpha/dt$) were determined at a specific cure time (t) by normalizing the partial heat of reaction ($\Delta H(t)$), and heat flow (dH/dt) by the total heat of reaction (ΔH), respectively:

$$\alpha = \frac{\Delta H(t)}{\Delta H} \tag{1}$$

$$\frac{d\alpha}{dt} = \frac{dH/dt}{\Delta H} \tag{2}$$

The cure kinetic parameters for the *n*th order with Borchardt–Daniels, autocatalytic model with Borchardt–Daniels, ASTM E698, and modified autocatalytic methods were extracted from the cure and cure rate data using linear least-squares fitting routines programmed in MATLAB. The resulting kinetic parameters were then used to predict and compare dynamic cure with experimental data at four different heating rates. To further validate the methods for isothermal cure, isothermal DSC runs were conducted at 120°C for different times. A cure temperature of 120°C was representative of PF cure under typical hot-pressing conditions for the panel core[1] and it also allowed easy observation of cure development with DSC. The DSC cell was preheated to 120°C and ~ 13.5 mg of PF resin was inserted and cured for different times. The sample was then quickly removed from the DSC and quenched in liquid nitrogen. The residual heat of reaction of the partially cured samples (ΔH_R) was obtained from a subsequent ramp scan at 10°C/min from 25 to 250°C. The time dependence of the degree of cure at 120°C was obtained by normalizing the difference of total and residual heat of reaction with total heat of reaction [$\alpha = (\Delta H - \Delta H_R)/\Delta H$] as a function of cure time. The total heat of reaction was taken as the average reaction heat previously measured in dynamic tests of fresh resins. The time dependence of the degree of cure at 120°C was compared with predictions from the MF methods.

Model-fitting algorithms

During a reaction process, the overall reaction rate can be modeled as:

$$\frac{d\alpha}{dt} = A\ \exp(-E/RT) f(\alpha) \tag{3}$$

where t (s) is the time, A (s^{-1}) the pre-exponential factor, E (J/mol) the activation energy, R (8.314 J/mol K) the universal gas constant, T (K) the absolute temperature, and $f(\alpha)$ the reaction model. Two reaction models are commonly used for simple reactions; these are the *n*th order $f(\alpha) = (1 - \alpha)^n$ and the autocatalytic model $f(\alpha) = \alpha^m(1 - \alpha)^n$ in which $m + n$ is called the order of reaction. Under isothermal conditions, in *n*th order kinetics, the rate of conversion is proportional to the concentration of unreacted material. Reaction rate therefore reaches its maximum at the onset of reaction and then decreases until the reaction is complete.[13] In autocatalyzed kinetics on the other hand, both the reactant and product are catalysts so that a maximum reaction rate is obtained during the course of the reaction.[8] Both models can be applied to dynamic experiments.[17]

Using the nth order and autocatalytic models, eq. (3) can be rearranged into eqs. (4) and (5) respectively:

$$\ln\left(\frac{d\alpha}{dt}\right) = \ln(A) + n\ \ln(1-\alpha) - \frac{E}{RT} \tag{4}$$

$$\ln\left(\frac{d\alpha}{dt}\right) = \ln(A) + m\ \ln(\alpha) + n\ \ln(1-\alpha) - \frac{E}{RT} \tag{5}$$

From one DSC dynamic scan, the values of α and $d\alpha/dt$ and corresponding temperature are used to solve eqs. (4) and (5) by multiple linear regression. Kinetic parameters A, E, and n for the nth order model (nth-BD) and A, m, n, and E for the autocatalytic model (Auto-BD) are thus determined.[13,18] This DSC analysis is usually designated as the Borchardt–Daniels method or the single heating rate method; it is attractive because all the kinetic parameters are derived from one single dynamic DSC scan. With this method however, kinetics parameters are heating rate dependent and they are subject to signal noise, solvent effect, and unresolved baselines.[19]

The kinetic parameters can also be determined from multiple heating rate scans. Specifically, in the case of a constant heating rate, $\beta = dT/dt$, eq. (3) can be rearranged into the integral form $g(\alpha)$:

$$g(\alpha) = \int_0^\alpha \frac{d\alpha}{f(\alpha)} = \frac{A}{\beta}\int_{T_0}^{T} \exp(-E/RT)\ dT \tag{6}$$

Because eq. (6) has no exact analytical solution, Doyle[20,21] proposed two approximations for $g(\alpha)$, which can be rearranged into:[22,23]

$$\ln\left(\frac{\beta}{T^2}\right) = \ln\left(\frac{RA}{Eg(\alpha)}\right) - \frac{E}{RT} \tag{7}$$

$$\log(\beta) = \log\left(\frac{AE}{R}\right) - \log g(\alpha) - 2.315 - \frac{0.4567E}{RT} \tag{8}$$

The peak temperature ($T_{i\text{peak}}$) dependency on heating rate (β_i) can thus be used to calculate the activation energy.[24,25] Assuming an isofractional peak temperature,[26–28] a linear regression of $\ln(\beta_i/T^2_{i\text{peak}})$ or $\log(\beta_i)$ against $1/T_{i\text{peak}}$ across several heating rates yields the activation energy with Kissinger eq. (9)[29] or Ozawa eq. (10),[22,25] respectively.

$$E = \frac{Rd[-\ln(\beta/T^2_{\text{peak}})]}{d(1/T_{\text{peak}})} \tag{9}$$

$$E = -2.19R\frac{d(\log\beta)}{d(1/T_{\text{peak}})} \tag{10}$$

Ozawa equation yields slightly higher E values than those obtained by Kissinger equation.[14,15] The calculated activation energy by Ozawa equation can be refined as suggested by ASTM E698 to be comparable with that by Kissinger equation. This modified version of Ozawa equation is designated as E698 method. For PF resins, Alonso et al.[15] found less than 4% variation in the estimates of E between the two equations. In addition, the estimates of E by E698 method are lower than those from the Borchardt–Daniels method.[15,30] To calculate the pre-exponential factor A, a definite reaction model must be assumed. For nth order reactions, Kissinger[29] proposed:

$$A = \frac{\beta E\ \exp(E/RT_{\text{peak}})}{RT^2_{\text{peak}}n(1-\alpha_{\text{peak}})^{n-1}} \tag{11}$$

Assuming a first order reaction, A is easily obtained from eq. (11) by substituting the intermediate heating rate and its corresponding peak temperature. Hence, with the E698 method, E can be determined regardless of the reaction model, while A can only be measured for nth order reactions.

Another method has been developed to calculate autocatalytic kinetic parameters from multiple heating rate DSC scans.[6,31,32] This method assumes that the degree of cure at the exothermic peak (α_{peak}) is heating rate-dependent and relates to the reaction orders m and n. The relationship between degree of cure at peaks and reaction orders is given by setting the optimum criteria in eq. (5):

$$m = \frac{\alpha_{\text{peak}}}{1-\alpha_{\text{peak}}}n. \tag{12}$$

For any specific kinetic process, α_{peak} is obtained experimentally, thus constraining the values of m and n by eq. (12). Another constraint arises from the integral function for the autocatalytic model in eq. (13):

$$g(\alpha) = \int_0^\alpha \frac{d\alpha}{\alpha^m(1-\alpha)^n} \tag{13}$$

In this case, the zero value of lower limit of integral imposes a constraint: m must be less than unity for $g(\alpha)$ to be finite.[17] It is possible to obtain a unique analytical solution for $g(\alpha)$ when $(n + m)$ sums to an integer higher than 1 and when $m < 1$.[17] However, for $n + m = 1$, the kinetic integral $g(\alpha)$ has different solutions for each value of n with $m < 1$.[17] In this article, $g(\alpha_{\text{peak}})$ is not solved analytically but rather numerically by assuming a value for the reaction order $m + n$ of 1, 2, and 3 respectively, within the constraints of eq. (12) and that of $m < 1$. Activation energy and pre-exponential factor are then determined simultaneously from the slope and intercept of the $\log(\beta_i) + \log[g(\alpha_{i\text{peak}})]$ versus $1/T_{i\text{peak}}$ plot across several heating rates β_i according to eq. (8). This method designated as the modified autocatalytic model (M-Auto) is advanta-

TABLE I
Summary of Kinetic Models, Parameters, and Methods Used

Method name	Model $f(\alpha)$	Kinetic parameters	Method used to extract kinetic parameters
E 698	First order $(1 - \alpha)$	A, E	ASTM E 698, multiple heating rates
nth-BD	nth order $(1 - \alpha)^n$	A, E, n	ASTM E 2041, single heating rate with Borchardt–Daniels method
Auto-BD	Autocatalytic model $\alpha^m(1 - \alpha)^n$	A, E, m, n	Single heating rate with Borchardt–Daniels method
M-Auto	Autocatalytic model $\alpha^m(1 - \alpha)^n$	A, E, m, n	Multiple heating rates

geous in that the peak temperature is not assumed isofractional.[6] Table I summarizes the mathematical expressions, parameters, and algorithms associated with each of the models used in this article.

RESULTS

PF cure analysis

The commercial PF resins exhibit two distinct exotherms that shift to higher temperatures with increasing heating rate (Fig. 1). PF-high displays an additional exothermic shoulder between the two major exotherms (Fig. 1). In PF-high, the highest molecular weight fractions react rapidly so that the maximum exotherm appears early for PF-high.[33] The PF-high resin reaches similar degree of cure at about 10°C earlier than that required for the PF-low resin (Fig. 1). As expected, DSC appears sensitive to differences in reaction exotherms and cure development of different resins.

Similar values for the total heat of reaction (ΔH) are measured at all heating rates for each resin. As expected, the more advanced PF-high resin releases less heat corresponding to the cure reaction (365 $\pm$ 5 kJ/kg) than does the PF-low resin (420 $\pm$ 9 kJ/kg) (Table I). In addition, the peak temperatures were found to be approximately isofractional regardless of heating rate (Table II).

Kinetic parameters from model-fitting kinetics

Table III summarizes the kinetic parameters obtained by the MF kinetics from dynamic test data for the two PF resins. The Auto-BD leads abnormal kinetic parameters and is therefore not applicable for PF resins. The Auto-BD method is unable to account for all intrinsic properties of the autocatalytic model, i.e., the constraints of m and n [eqs. (12) and (13)] are not met with this method.

The nth-BD, E698, and M-Auto methods generate consistent activation energies and pre-exponential factors for both resins (Table III). These parameters are in the 83–105 kJ/mol and 19–26 s^{-1} ranges respectively, and are in agreement with the literature[9] and with model-free kinetics methods.[7] With all three methods, slightly higher activation energy is found for PF-high than that for PF-low, consistent with the higher advancement of PF-high.[11]

The advantage of the E698 and M-Auto methods over the nth-BD method is that kinetic parameters can be determined for individual exotherm. The M-Auto method is only applicable when a reaction order (m) is small. When the M-Auto method can be applied, it generates activation energies slightly lower than those measured with the E698 method (Table III). Recall that the E698 method neglects the dependence of α_{peak} on heating rates, whereas this dependence is included in the M-Auto method.[6] For the two PF resins used in this study, there are only small variations for degree of cure at peaks across heating rates. As a result, both methods lead to small differences in activation energies for the two resins. The nth-BD method gives cure kinetic parameters for the overall cure process at each heating rate, which are very similar to those obtained from maximum peaks with E698. A trend toward higher activation energies with increasing heating rates for

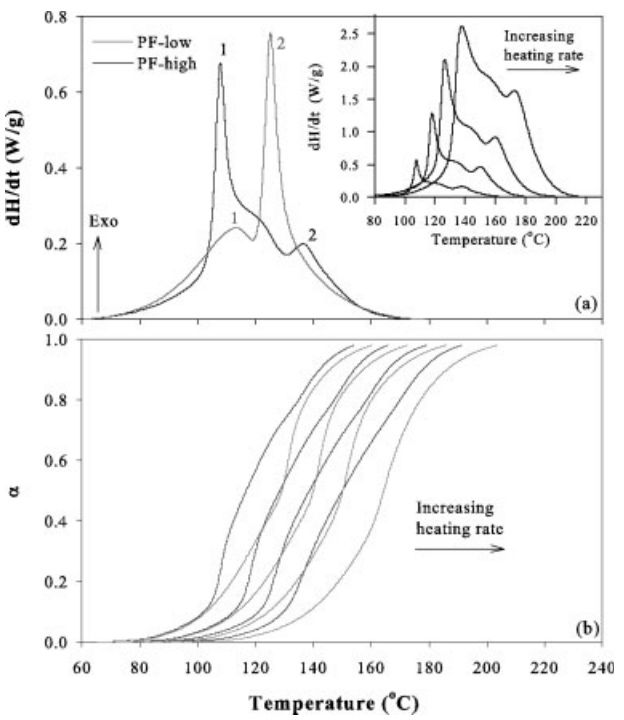

Figure 1 (a) DSC heat flow (dH/dt) at 2°C/min and (b) degree of cure (α) for PF-low and PF-high. The numbers 1 and 2 designate exotherm peaks 1 and 2. Inset in (a) highlights the influence of heating rates (2, 5, 10, and 20°C/min) on the cure of PF-high.

TABLE II
Summary of PF Cure Peak Temperature, Degree of Cure at Peaks in Parentheses, and Heat of Reaction Across Four Heating Rates[a]

	β (°C/min)	2	5	10	20
PF-low	T_1 (°C) (α_1)	119 (0.31)	130 (0.30)	137 (0.29)	153 (0.26)
	T_2 (°C) (α_2)	131 (0.59)	142 (0.57)	151 (0.54)	163 (0.46)
	ΔH (kJ/kg)	406	427	425	424
PF-high	T_1 (°C) (α_1)	108 (0.23)	118 (0.23)	128 (0.24)	135 (0.19)
	T_2 (°C) (α_2)	137 (0.82)	149 (0.83)	159 (0.81)	169 (0.78)
	ΔH (kJ/kg)	365	363	373	361

[a] Six replicates, the standard error $\leq$ 2.65 for all variables.

the PF-low resins is observed (Table III). The higher activation energies measured at 20°C/min suggest that this heating rate is less appropriate to characterize PF cure. This discrepancy is likely due to the higher thermal lag manifested at the higher heating rate. The *n*th-BD method is generally observed to overestimate the kinetic parameters when compared with the E698 method.[15,30] However, with the exception of the 20°C/min, this overestimate is not apparent in this study. It is clear that the *n*th-BD and E698 methods can provide consistent kinetic parameters, and the M-Auto method is limited to small reaction orders while the Auto-BD method is inapplicable.

Predicting cure for dynamic conditions

Dynamic cure development was predicted by substituting values of activation energy, pre-exponential factor, reaction orders, and arbitrary heating rates for the corresponding *n*th order model or autocatalytic model into eq. (3). The equations were then solved using the Runge–Kutta method[34] implemented in a MATLAB program. All kinetic parameters from Table III can be used to predict cure behavior. Further, with the E698 method two reactions can be modeled as independent and consecutive reactions [eq. (14)].[23] Two reactions can also be modeled as parallel and competing [eq. (15)].[35] In both cases, the overall reaction rate is obtained by substituting the kinetic parameters obtained from individual peaks 1 and 2 as indicated by the subscripts in eqs. (14) and (15).

$$\frac{d\alpha}{dt} = w_1 \frac{d\alpha_1}{dt} + w_2 \frac{d\alpha_2}{dt} = w_1 A_1 \exp\left(\frac{-E_1}{RT}\right)(1-\alpha_1) + w_2 A_2 \exp\left(\frac{-E_2}{RT}\right)(1-\alpha_2) \quad (14)$$

$$\frac{d\alpha}{dt} = A_1 \exp\left(\frac{-E_1}{RT}\right)(1-\alpha) + A_2 \exp\left(\frac{-E_2}{RT}\right)(1-\alpha) \quad (15)$$

where w_i is the fraction of each reaction. In this study peak deconvolution allowed an estimate of relative heat of reaction for the two main exotherms at around $w_i = 0.5$. Within E698 method, predictions are compared with parameters (A, E) obtained for peaks 1 and 2 respectively, and also compared with combinations of two distinct exotherms as described in eqs. (14) and (15). The predictions are best when two independent or consecutive reactions [eq. (14)] are assumed as indicated by the lowest mean squared error of prediction[36] (MSEP).

TABLE III
Kinetic Parameters for the PF-Low and PF-High Resins Obtained from the Model-Fitting Kinetic Methods

			PF-low			PF-high			
Method			E (kJ/mol)	ln A (1/s)	n	E (kJ/mol)	ln A (1/s)	n	R^2
*n*th-BD[a]		2°C/min	94	22	1.15	99	24	1.14	≥ 0.93
		5°C/min	96	23	1.15	99	24	1.13	
		10°C/min	99	23	1.11	99	24	1.13	
		20°C/min	104	25	1.18	105	25	1.23	
E 698		Peak 1	87	21	1.00	99	26	1.00	≥ 0.99
		Peak 2	97	23	1.00	98	23	1.00	
M-Auto	Peak1	$m + n = 1$	83	19	0.71	94	23	0.78	≥ 0.99
	Peak1	$m + n = 2$	84	20	1.42	96	24	1.55	
Auto-BD[a]		5°C/min	15	−1	0.82	−1	−6	0.66	≥ 0.93

[a] Average of four replicates at each heating rate, standard deviation $\leq$ 2.90.

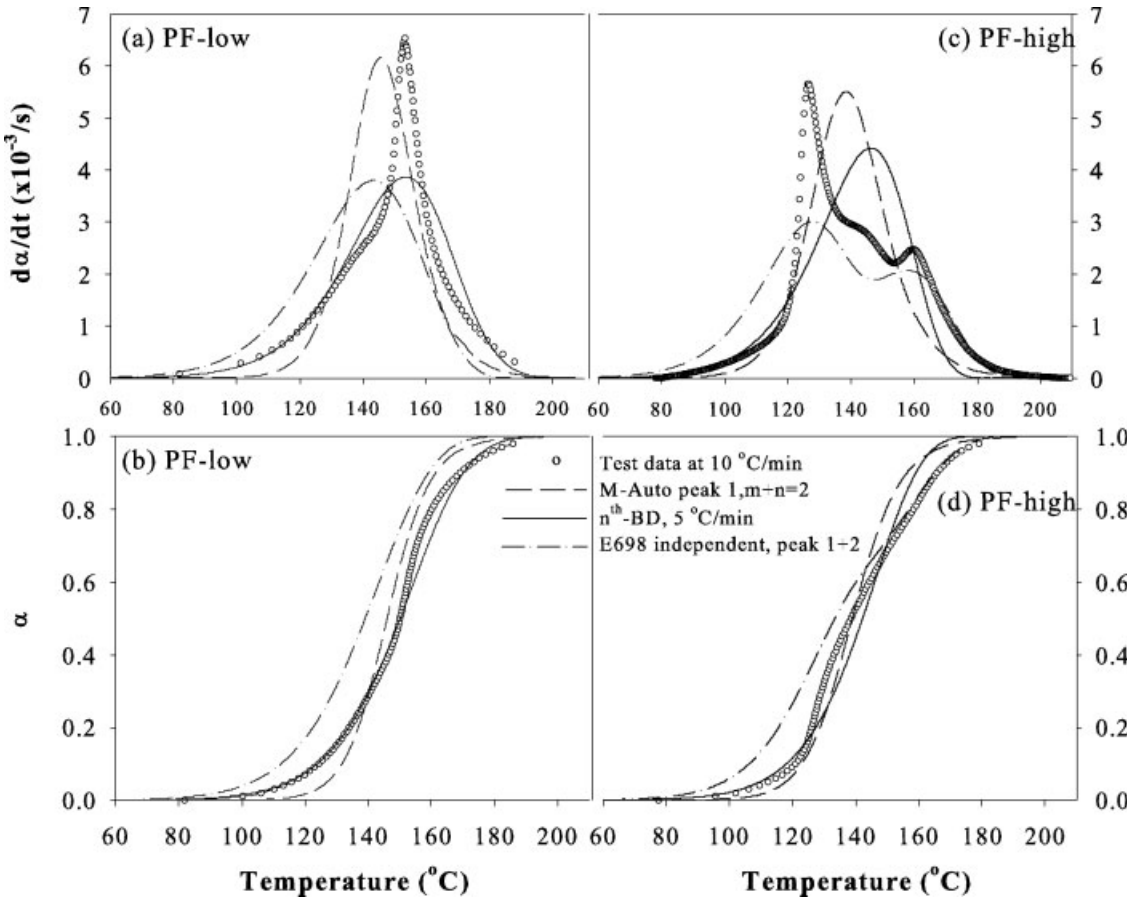

Figure 2 Comparison of the test data at 10°C/min and MF predictions of PF-low and PF-high for reaction rate ($d\alpha/dt$) and degree of cure (α).

Figure 2 shows the test data and predictions of reaction rate and degree of cure for both resins by parameters from each one of the E698, *n*th-BD, and M-auto methods, which are best among each method as evidenced by the lowest MSEP in Table IV. Clearly, the MF kinetic models studied predict the degree of cure for PF resins better than the reaction rate. The failure to accurately model reaction rate of PF cure likely stems from the limitation of most MF kinetics to one reaction and the fact that PF cure involves multiple reactions as evidenced by the multiple exotherms in the PF-low and PF-high thermograms. When two independent or consecutive reactions [eq. (14)] are assumed with E698 method, two peaks are captured for the reaction rate of PF-high [Fig. 2(c)]. This method also predicts PF-high degree of cure very accurately after 70% conversion [Fig. 2(d)]. Over the entire cure process however, the *n*th-BD method produces the best predictions of degree

TABLE IV
Mean Squared Errors of Prediction (MSEP) for Both Dynamic and Isothermal Conditions at Specific Degree of Cure and Data Points (in Parentheses)

Predicted variable	Model	PF-low	PF-high
Dynamic (10°C/min) temperature at α (°C)[2]	M-Auto peak 1, $m + n = 2$	51.2 (99)	40.1 (99)
	*n*th-BD, 5°C/min	4.6 (99)	14.9 (99)
	E 698 independent, peak 1 + 2	128.7 (99)	63.9 (99)
	Model-free kinetics KAS	3.0 (99)	0.30 (99)
Dynamic (10°C/min) reaction rate at α (10^{-6}) (1/s) [2]	M-Auto peak 1, $m + n = 2$	1.8 (99)	2.0 (99)
	*n*th-BD, 5°C/min	2.1 (99)	1.9 (99)
	E 698 independent, peak 1 + 2	2.6 (99)	0.6 (99)
	Model-free kinetics KAS	0.1 (99)	0.06 (99)
Isothermal (120°C) cure time at α (min) [2]	M-Auto peak 1, $m + n = 2$	67.9 (11)	55.1 (13)
	*n*th-BD, 5°C/min	32.4 (11)	11.5 (13)
	E 698 independent, peak 1 + 2	68.6 (11)	24.0 (13)
	Model-free kinetics KAS[7]	12.0 (11)	19.4 (13)

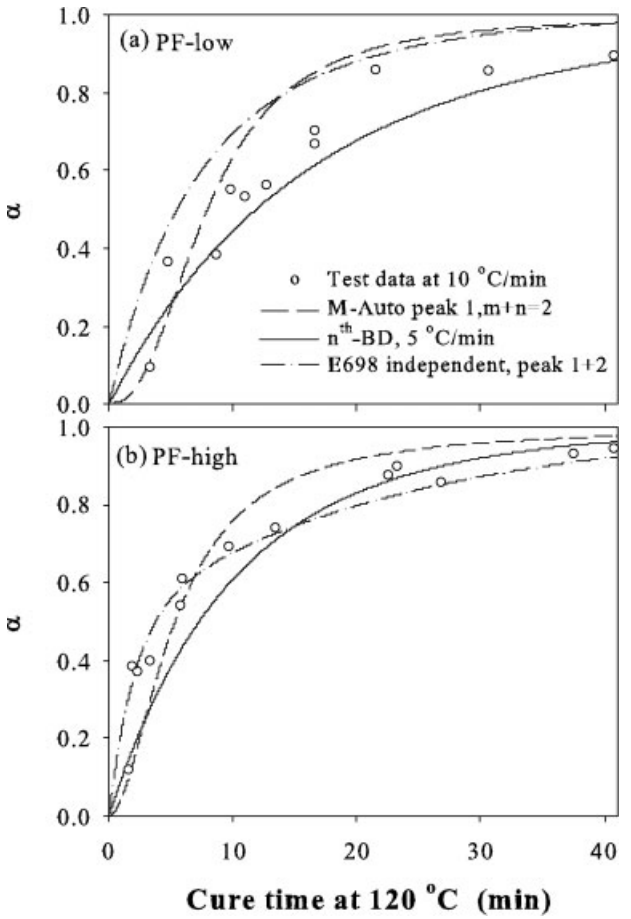

Figure 3 Experimental degree of cure (α) at 120°C and MF predictions for (a) PF-low and (b) PF-high.

of cure as evidenced by the lowest MSEP (Table IV). This is true for both resins. As a conclusion, none of the models evaluated accurately predict the reaction rate of the PF cure studied. However, the degree of cure is accurately predicted with the *n*th-BD method. But the MSEP values for this method are higher than those obtained with the model-free kinetics Kissinger–Akahira–Sunose (KAS) method in a parallel study.[7] This indicates that overall, model-free kinetics methods are better than MF method for dynamic predictions.

Predicting cure for isothermal conditions

The ability to predict isothermal cure from dynamic scan data is significant because dynamic tests are more repeatable and easily conducted compared to isothermal tests. In addition, such predictions provide further validation of the models. The predictions of isothermal cure development from all three models are compared to experimental data in Figure 3. For PF-low, *n*th-BD is more accurate than others [Fig. 3(a)]. However, for PF-high, the E698 with an assumption of two independent reactions [eq. (14)] is more accurate during the early curing period, while *n*th-BD predicts a little better toward the end of cure. Across the cure regime studied, the *n*th-BD model performs better as evidenced by MSEP (Table IV). Generally, *n*th-BD method is the best prediction model of isothermal cure. Comparing with model-free kinetics KAS method in a parallel study,[7] the MSEP with *n*th-BD is the same order with that by KAS for PF-high, and higher for PF-low (Table IV); supporting the notion that the model-free kinetics KAS model is more accurate for isothermal prediction than *n*th-BD method.

SUMMARY AND CONCLUSIONS

The applicability of model-fitting kinetics for predicting cure development of PF resins is compared. The Auto-BD is inappropriate for kinetic modeling of commercial PF resins. The activation energy obtained by *n*th-BD, E698, and M-Auto methods are comparable. All methods give inaccurate predictions of reaction rate while providing reasonable predictions for degree of cure in both dynamic and isothermal conditions. For a high molecular weight PF resin, the E698 independent method provides an excellent local prediction of degree of cure above 70% under dynamic conditions, and works better at the early curing period under isothermal conditions. Altogether, the *n*th-BD method performs better than the other methods. Yet, the *n*th-BD predictions are not as good as those by model-free kinetics. On the other hand, they can be easily incorporated in a complex hot-pressing model. Considering that *n*th-BD method requires only one single heating rate, this method is recommended for simple kinetic modeling of PF resins.

The authors would like to dedicate this article to our late colleague and friend, Dr. Balázs G. Zombori.

References

1. Zombori, B. G.; Kamke, F. A.; Watson, L. T. Wood Fiber Sci 2004, 36, 159.
2. Bolton, A. J.; Humphrey, P. E. Holzforshung 1988, 42, 403.
3. Thoemen, H.; Humphrey, P. E. Wood Fiber Sci 2003, 35, 456.
4. Dai, C.; Yu, C.; Wood Fiber Sci 2004, 36, 585.
5. Luukko, P.; Alvila, L.; Holopainen, T.; Rainio, J.; Pakkanen, T. T. J Appl Polym Sci 2001, 82, 258.
6. Harper, D. P.; Wolcott, M. P.; Rials, T. G. Int J Adhes Adhes 2001, 21, 137.
7. Wang, J.; Laborie, M. P. G.; Wolcott, M. P. Thermochim Acta 2005, 439, 68.
8. Prime, R. B. In Thermal Characterization of Polymeric Materials, 2nd ed.; Turi, E. A., Ed.; Academic Press: New York, 1997; Chapter 6.
9. Kay, R.; Westwood, A. R. Eur Polym J 1975, 11, 25.
10. Rials, T. G. ACS Symp Ser 489 1992, 282.
11. Vázquez, G.; González-Álvarez, J.; López-Suevos, F.; Freire, S.; Antorrena, G. J Therm Anal Cal 2002, 70, 19.
12. Park, B.-D.; Riedl, B.; Kim, Y. S.; So, W. T. J Appl Polym Sci 2002, 83, 1415.

13. ASTM E2041-03, ASTM International: West Conshohocken, USA
14. ASTM E 698-01, ASTM International: West Conshohocken, USA
15. Alonso, M. V.; Oliet, M.; Pérez, J. M.; Rodríguez, F; Echeverría, J. Thermochim Acta 2004, 419, 161.
16. Nelson, D. W.; Sommers, L. E. In Methods of Soil Analysis, Part 2: Chemical and Microbiological Properties, 2nd ed.; Page, A. L., Ed.; American Society of Agronomy: Madison, WI, 1982; Chapter 29.
17. Martin, J. L.; Salla, J. M. Thermochim Acta 1992, 207, 279.
18. Borchardt, H. J.; Daniels, F. J Am Chem Soc 1957, 79, 41.
19. Dunne, R. C.; Sitaraman, S. K.; Luo, S.; Rao, Y.; Wong, C. P.; Estes, W. E.; Gonzalez, C. G.; Coburn, J. C.; Periyasamy, M. J Appl Polym Sci 2000, 78, 430.
20. Doyle, C. D. J Appl Polym Sci 1961, 5, 285.
21. Doyle, C. D. J Appl Polym Sci 1962, 6, 639.
22. Ozawa, T. Bull Chem Soc Jpn 1965, 38, 1881.
23. Flynn, J. H.; Wall, L. A. J Res Natl Bur Stand Sect A 1966, 70, 487.
24. Kissinger, H. E. J Res Natl Bur Stand Sect A 1956, 57, 217.
25. Shulman, G. P.; Lochte, H. W. J Macromol Sci Chem 1968, 2, 411.
26. Horowitz, N. H.; Metzger, G. Anal Chem 1963, 35, 1464.
27. Prime, R. B. Polym Eng Sci 1973, 13, 365.
28. Wang, Y.-H.; Hong, Y.-L.; Hong, J.-L. J Appl Polym Sci 1995, 58, 1585.
29. Kissinger, H. E. Anal Chem 1957, 29, 1702.
30. Park, B.-D.; Riedl, B.; Hsu, E. W.; Shields, J. Polymer 1999, 40, 1689.
31. Lam, P. W. K. Polym Compos 1987, 8, 427.
32. Chung, T. S. J Appl Polym Sci 1984, 29, 4403.
33. Detlefsen, W. D. In Surfaces, Chemistry and Applications; Chaudhury, M.; Pocius, A. V., Eds.; Elsevier: Amsterdan, 2002; Chapter 20.
34. Dormand, J. R.; Prince, P. J. J Comput Appl Math 1980, 6, 19.
35. Vyazovkin, S. J Comput Chem 2001, 22, 178.
36. Rawlings, J. O.; Pantula, S. G.; Dickey, D. A. Applied Regression Analysis, 2nd ed.; Springer: New York, 1998.